Aridity and cold temperatures drive divergent adjustments of European beech xylem anatomy, hydraulics and leaf physiological traits

Eduardo Vicente, Margaux Didion-Gency, Luna Morcillo, Xavier Morin, Alberto Vilagrosa, Charlotte Grossiord

Aridity and cold temperatures drive divergent adjustments of European beech xylem anatomy, hydraulics, and leaf physiological traits

Eduardo Vicente[1, 2]*, Margaux Didion-Gency[3], Luna Morcillo[2], Xavier Morin[4], Alberto Vilagrosa[2], Charlotte Grossiord[5, 6]

[1]IMEM Ramón Margalef, Departament of Ecology, Faculty of Sciences, University of Alicante, 03080, Alicante, Spain

[2]CEAM Foundation, Joint Research Unit University of Alicante-CEAM, Dept Ecology, University of Alicante, PO Box 99, 03080, Alicante, Spain.

[3]Ecosystem Ecology, Forest Dynamics Unit, Swiss Federal Institute for Forest, Snow and Landscape WSL, Zürcherstrasse 111, 8903, Birmensdorf, Switzerland

[4]CEFE UMR 5175 (CNRS, Université de Montpellier, Université Paul-Valéry Montpellier, EPHE, IRD), 1919 Route de Mende, F-34293, Montpellier Cedex 5, France

[5]Plant Ecology Research Laboratory PERL, School of Architecture, Civil and Environmental Engineering, EPFL, Lausanne, CH-1015, Switzerland

[6]Functional Plant Ecology, Community Ecology Unit, Swiss Federal Institute for Forest, Snow and Landscape WSL, Lausanne, CH-1015, Switzerland.

*Corresponding author. E-mail address: ev.bartoli@ua.es

Abstract

Understanding plant trait coordination and variance across climatic gradients is critical for assessing forests' adaptive potential to climate change. We measured eleven hydraulic, anatomical and leaf-level physiological traits in European beech (*Fagus sylvatica* L.) along a moisture and temperature gradient in the French Alps. We assessed how traits covaried, and how their population-level variances shifted along the gradient. The intrapopulation variances of vessel size and xylem-specific conductivity reduced in colder locations as narrow vessels were observed in response to low temperature. This decreased individual-level water transport capacity compared to the warmer and more xeric sites. Conversely, the maximum stomatal conductance and Huber value variances were constrained in the arid and warm locations, where trees showed restricted gas exchange and higher xylem-specific conductivity. The populations growing under drier and warmer conditions presented wide variance for the xylem anatomical and hydraulic traits. Our results suggest that short-term physiological acclimation to raising aridity and heat in southern beech populations may occur mainly at the leaf level. Furthermore, the wide variance of the xylem anatomical and hydraulic traits at these sites may be advantageous since more heterogeneous hydraulic conductivity could imply populations' greater tree-tree complementarity and resilience against climatic variability. Our study highlights that both intrapopulation trait variance and trait network analysis are key

approaches for understanding species adaptation and the acclimation potential to a shifting environment.

Keywords: Intraspecific trait variation, trait coordination, trait variances, water use, climatic stress, xylem hydraulics, leaf physiology.

Introduction

Understanding acclimation processes in trees is crucial for predicting forest dynamics under novel stressful conditions linked with climate change. Dysfunctions in tree water relations and hydraulic efficiency are globally correlated with climate-associated forest decline and mortality (McDowell et al. 2008, Klein 2015, Anderegg et al. 2016). Thus, forest health very much depends on trees' capacity to modulate their water-use strategies to a changing environment (Messier et al. 2018). In this context, functional traits related to xylem anatomy, hydraulic conductivity and leaf-level water use emerge as key proxies of tree water-use economy (Gleason et al. 2013, Anderegg 2015).

Variation in the functional traits that regulate water use has been widely assessed along environmental gradients to identify adaptive patterns. As climate goes from wetter to drier conditions, trees tend to shift from an acquisitive to a conservative water-use strategy (Reich 2014). For instance, xeric environments promote the formation of narrower xylem vessels (e.g. García-Cervigón et al. 2018, López et al. 2021). Trees from dry environments also tend to optimise water supply to functional leaves, which is consistently observed across species as an increment in Huber value (i.e. the ratio of stem section per leaf area unit) (Martínez-Vilalta et al. 2009, Gleason et al. 2013, Pritzkow et al. 2019, Rosas et al. 2019). Additionally, the gas exchange rates of trees growing in more arid conditions are usually lower (i.e. stomatal conductance and assimilation capacity), and their water-use efficiency increases to prevent

leaf hydraulic damage (Aranda et al. 2015, Lübbe et al. 2017, Torres-Ruiz et al. 2019, Henry et al. 2019).

Temperature is also a primary driver of variation in water-use-related functional traits. Rising temperatures lead to high vapour pressure deficit (VPD), which increases the dehydration risk (Kurz et al. 2008, Will et al. 2013). Plants tend to mitigate heat impacts by performing stronger stomatal control and reducing their whole-tree hydraulic conductance (Bréda et al. 2006, Grossiord et al. 2020). Low temperatures can trigger frost-induced cavitation in temperate and cold ecosystems (Mayr et al. 2003, Charrier et al. 2017). As an adaptation mechanism to this disturbance in cold environments, trees promote narrower vessels (Castagneri et al. 2015, Schreiber et al. 2015, García-Cervigón et al. 2020), similarly to when they are subjected to dry conditions. Trees exposed to frequent frosts and longer winters have higher maximum assimilation rates compared to those growing under milder temperature conditions (Huxman et al. 2008, Bresson et al. 2011).

However, there are still many uncertainties about the intraspecific trait variation dimension in response to environmental variability in trees because current knowledge is based mainly on interspecific comparisons. Yet, intraspecific trait variability can be wider than interspecific variability (e.g. Jung et al. 2014, Siefert et al. 2015). Furthermore, interspecific adaptive patterns to shifting environments can vastly vary within species (Lübbe et al. 2017, Fuchs et al. 2021), which indicates the need for more studies to assess intraspecific trait variability. Moreover, most existing studies have addressed trait variation by a univariate approach, although functional traits involved in water use normally show consistent correlations (i.e. trait coordination). Indeed vessel anatomy is closely coupled with hydraulic conductivity (Zimmermann 2002, Sperry et al. 2008). The latter has been positively related to greater stomatal conductance and leaf-level water use (Brodribb et al. 2002, Brodribb and Holbrook 2003). In this context, studying trait covariation using coordination networks has been

suggested to gain more mechanistic insights into adaptive processes (Poorter et al. 2014, Messier et al. 2017). The emergence of covariation structures would depict the selection of specific trait combinations in response to climate shifts. However, the trait coordination structures observed across species do not necessarily hold within species (Umaña and Swenson 2019, Rosas et al. 2019). Furthermore, recent studies conducted on an intraspecific scale suggest that trait coordination may vastly vary depending on climate conditions (Carvalho et al. 2020, Benavides et al. 2021). So it is necessary to better understand how traits are coordinated within species and along environmental gradients.

In addition to adjustments to trait values and coordination, understanding how trait variance patterns are distributed across a given species' populations might be essential for predicting its adaptive potential (Ahrens et al. 2021). Indeed population-level heritable trait plasticity can be modified due to local adaptations (Linhart and Grant 1996, Valladares et al. 2007, 2014). For instance, stressful climate conditions can filter out unfavourable trait values (i.e. climatic filtering effect) which, in turn, reduces community-level trait variance (Weiher et al. 1995, Swenson and Enquist 2007). Such reductions in pools of available trait variances can limit population adjustment capacity (Molina-Montenegro and Naya 2012, Anderegg et al. 2020). In this context, studies performed on an interspecific scale report narrow variances for woody traits (i.e. wood density and bark thickness) in communities growing under cold conditions (Swenson et al. 2012), and the same applies to leaf anatomical traits in water-limited environments (Swenson et al. 2012, Šímová et al. 2017). Within species, Anderegg et al. (2020) observed constrained variance patterns for leaf dry mass content in more xeric populations. Nonetheless, very few studies have addressed intraspecific trait variance patterns along broad climatic gradients, and current knowledge on their climatic drivers is still weak (Šímová et al. 2017, Anderegg et al. 2020).

In order to improve our understanding of intraspecific water-use strategy variation, our study focuses on European beech (*Fagus sylvatica* L.). Beech is a widely distributed species in European forests. It is quite sensitive to both drought (Geßler et al. 2007, Friedrichs et al. 2009) and temperature extremes (Weigel et al. 2018, Gazol et al. 2019), which makes it a key species for understanding trait adjustments along climatic gradients. Specifically, we centre on xylem anatomy (i.e. vessel size and density), hydraulics (i.e. maximum xylem- and leaf-specific conductivity, loss of conductivity, Huber value) and leaf physiology (i.e. stomatal conductance, assimilation rate, water-use efficiency) traits. Our study area lies along a 300 kilometre-long precipitation and temperature gradient in the southern French Alps. The gradient covers an extensive geographical range from the southern Mediterranean edge to the wetter alpine limit of beech, where heat+aridity and low temperature are, respectively, its main limiting factors. Our objectives are to assess: (i) how the functional traits that modulate beech water use vary in different climates along the gradient; (ii) how coordination among these functional traits varies along the climatic gradient; (iii) whether their population-level variance is constrained by aridity+heat or low temperature. We hypothesise that: (1) towards colder climates, beech trees reduce vessel size and maximum hydraulic conductivity because of frost risk, and show greater assimilation capacity consistently with a more acquisitive water-use strategy. Drier climates reduce vessel size, hydraulic conductivity and gas exchange capacity by promoting a conservative water-use strategy; (2) xylem anatomical traits are closely coordinated with hydraulic traits (i.e. a bigger vessel area should be associated with greater hydraulic conductivity) and the latter with gas exchange capacity (i.e. greater hydraulic conductivity linked with more leaf-level water use). This coordination varies depending on adjustments to aridity and low temperature; (3) aridity+heat or low temperature on both gradient edges reduces population-level trait variances because of climatic filtering.

Materials and Methods

Study area

This study was carried out at six sites scattered along a climatic gradient in the French Alps (Fig. 1) (Jourdan, Kunstler, et al. 2019, Jourdan, Lebourgeois, et al. 2019, Jourdan et al. 2021). The mean annual precipitation and temperature among the sites along the south to north gradient range from 877 mm to 1,292 mm and from 11ºC to 6.7ºC, respectively. At the three most southern and driest sites (SB, LU, LA), forest type is composed mostly of beech and downy oak (*Quercus pubescens* Willd.), and of beech and silver fir (*Abies alba* Mill.) at the three northern sites (VT, VC, BG). A recent study along the same gradient depicts that there are no discrete genetic differences between sites, which suggests that they belong to the same genetic population (Capblancq et al. 2020). To reduce the impact of interspecific interactions, two monospecific plots were selected at each site consisting of a 17.5 metre-radius circle where at least 90% of the basal area is represented by beech. In each plot, five dominant trees were selected for sampling (10 trees per site, n=60 trees in all). All the plots along the gradient are north- or north-west oriented, and of a limestone bedrock type. The selected stands have not been managed in at least the last decade, and their structure is high forest in all the plots, except LU, where forest is coppice. The main attributes of each site are depicted in Table 1, and more details about site selection and characteristics can be found in Jourdan, Lebourgeois, et al. (2019) and Jourdan et al. (2020).

Field sampling and laboratory measurements

One field campaign per site was carried out between July and August 2019. Two 3-4 metre-long healthy top-of-canopy branches were harvested at predawn and midday from all the selected trees. Canopy was accessed with tree-climbing equipment in all the plots, except LU, where a telescopic pole pruner was used. Directly after branch cutting at predawn, leaf water

potential (Ψ_{pd}) was measured on one terminal leaf per branch by a Scholander pressure chamber (PMS Instrument Co., Corvallis, Oregon, USA).

From the branches harvested at midday, a terminal section of at least 1.5 m was immediately removed and placed in water, where it was recut at least twice to remove potential xylem cavitation effects. Afterwards, maximum stomatal conductance and assimilation rates (gs_{max} and A_{max}, respectively) were measured on one terminal leaf using an infrared gas-exchange analyzer (LI-COR 6400, LI-COR, Lincoln, USA). Measuring the gas exchange rates by this method had no impact on A_{max} and gs_{max} (Verryckt et al. 2020). Measurements were taken at the following settings in a 2×3 LED chamber: 400 ppm of reference CO_2 concentration, 1,500 µmol m^{-2} s^{-1} light-saturating photosynthetic photon flux density, 50% relative chamber humidity, and block temperature adjusted to 20°C or 30°C to match the ambient conditions at each site while measurements were taken (i.e. BG, VC, VT = 20°C, LA, LU, SB = 30°C). As the measured leaves covered the whole LI-COR 6400 cuvette, no correction for leaf area was conducted. Leaf temperature was measured using the energy balance. Data were recorded after the steady-state gas exchange rates had remained for at least 4 min. Intrinsic water-use efficiency (WUEi) was obtained by dividing A_{max} by gs_{max}.

Foliar carbon isotopic composition ($\delta^{13}C$, ‰), a proxy for water-use efficiency integrated over the entire period since leaves formed (Farquhar 1989, Ehleringer et al. 1993), was measured on the sunlight leaves taken from the same branches used for the gas exchange measurements. Leaf material was dried at 65°C for 48 h, Dried samples were finely ground. About 1 mg of the powdered material was placed inside tin capsules (Säntis, Teufen, Switzerland) for the $\delta^{13}C$ analysis. Measurements were taken on an elemental analyzer interfaced to a DeltaPlusXP isotope ratio mass spectrometer (EA-IRMS; Thermo EA 1100 Deltaplus XL; 0.1‰ precision) in the stable isotope research centre (SIRC) of WSL (Birmensdorf, Switzerland).

From every branch taken at midday, 20 centimetre-long shoots (approx. 70 cm from the apex, diameter between 2-5 mm) were taken and placed inside vials with 50% ethanol solution to determine wood anatomy. In the laboratory, 12 micrometre-width cross-sections were obtained from each sample using a Reichert Om E based microtome (Gärtner et al. 2014). Cross-sections were stained with safranine-astrablue (1% and 0.5% in distilled water, respectively), mounted on glass slides with Canada balsam, and dried in an oven at 60ºC for 24 h. Slides were photographed by a microscope Olympus BX41 at 40x magnification. Vessel diameter (D), vessel density (Vd) and relative vessel lumen area (i.e. vessel lumen to sapwood area ratio) (VA) were calculated by the ImageJ software. Xylem anatomical measurements were taken on the last two rings because this wood section is responsible for most twig water transport (Domec and Gartner 2002, Bouche et al. 2014). Vessel hydraulic diameter (i.e. the effective vessel diameter that contributes to hydraulic conductivity) was calculated according to (Sperry and Hacke 2004) as follows:

$$Dh = 2\left(\frac{\sum r^5}{\sum r^4}\right)$$

where r is the vessel radius in microns (μm).

A 1-metre terminal section was cut from every branch for the hydraulic traits measurements and immediately placed inside sealed dark plastic bags with wet tissue to maintain high moisture conditions. Samples were sent to the laboratory over the next 24 h, stored in a cold chamber at 5ºC, and processed within the next 2 or 3 days. The analysis was performed using a Xyl´em device (Bronkhorst, France) according to Cochard et al. (2005). Deionised, filtered and degassed water, with 1M and 10M concentrations of $CaCl_2$ and KCl, respectively, was used for the analysis. Eight small shoots were cut underwater from each branch and placed in a manifold. Then a low pressure (45kPa) flow was applied to measure the initial hydraulic conductivity of each shoot. Samples were flushed at 0.1 MPa for 3 minutes to remove any air bubbles that obstructed vessels. Previous tests determined that a maximum of 3 minutes

allowed all air bubbles to be removed, and the maximum hydraulic conductivity (Kh_f) could be recorded. The percent loss of conductivity (PLC) was calculated using the ratio of the initial hydraulic conductivity (Kh_i) recorded before flushing samples were divided by Kh_f, and expressed as percentage units as follows:

$$PLC = 100\left(1 - \frac{Kh_i}{Kh_f}\right)$$

Xylem-specific conductivity (Ks) was calculated for every shoot by dividing Kh_f by the sapwood area, estimated as the cross-section without bark. Simultaneously, leaf-specific conductivity (LSC) was calculated by dividing Kh_f by the leaf area associated with every shoot, measured using a LICOR scanner (LI-3100 Area Meter, LI-COR, USA). Huber value (HV) was estimated as the sapwood area/leaf area ratio.

All the measured traits and their units are summarised in Table 2.

Climate data

Climate data were obtained for each site from the current climate WorldClim database at ~1km^2 resolution grid from https://www.worldclim.org/data/index.html (Fick and Hijmans 2017). A set of the potential explanatory variables was selected for trait variability, which accounted for water availability and temperature effects (i.e. averages and extremes): mean annual precipitation (pp); mean minimum temperature of the coldest month (MTCM); mean maximum temperature of the warmest month (MTWM). For each site, the annual P/PET (precipitation/potential evapotranspiration) index from the layer available at http://www.cgiar-csi.org/data/global-aridity-and-pet-database was downloaded, which derives from the same WorldClim database.

263 Statistical analysis

264 We tested the correlation between the explanatory climate variables (pp, MTCM, MTWM,
265 P/PET) and found that they were highly correlated (i.e. Pearson's correlation coefficient higher
266 than 0.7 in all cases). We thus summarised the climate variables in a single variable by
267 performing a principal component analysis (PCA). The first obtained component, PC1,
268 explained 95% of variance. It was chosen as the best representative of the moisture and
269 temperature gradient. We performed Pearson's correlation analysis between PC1 and every
270 measured trait to assess the relations between climatic gradient and trait variability. The
271 normality for all the traits was previously tested by the Shapiro-Wilk test and was log-
272 transformed whenever necessary. Gaussian kernel density estimations were used to explore
273 the vessel diameter distribution among populations, following Schreiber et al. (2015) and
274 García-Cervigón et al. (2020). Kernel density estimation is a non-parametric procedure that
275 calculates the probability density function of a variable from a finite number of samples
276 (Silverman 1986). R function *density* was used for this purpose.

277 Coordination between traits was evaluated with path analyses using R-packages lavaan v.06-7
278 (Roseel 2012) and semplot v. 1.1.2 (Epskamp 2019). A first model was performed for all trees
279 and sites (i.e. general model) to characterise the trait coordination along the whole gradient.
280 To better assess the climate effect on the coordination network, and the gradual
281 differentiation between northern and southern populations (Capblancq et al. 2020), two more
282 models were carried out: one for the trees at our three southern, drier and warmer sites (i.e.
283 arid-warm model, PC1<0: SB, LU, and LA), and another for the trees at our three northern,
284 wetter and colder sites (i.e. wet-cold model, PC1>0: VT, VC, and BG). Path structures were built
285 by assuming direct relations among vessel hydraulic diameter (Dh), hydraulic conductivity (Ks
286 and LSC) and maximum stomatal conductance (gs_{max}), and by accounting for empirical
287 interactions between the traits of each group of traits (i.e. wood anatomy, xylem hydraulics,

288 leaf physiology). We eliminated the less significant paths stepwise until the best fitted and
289 predicted models were found (based on χ^2, RMSEA and CFI indices).

290 We also analysed the population-level trait variance for every site using the $T_{IC/IR}$ statistic
291 proposed by Violle et al. (2012) by taking each site as a different population. $T_{IC/IR}$ is calculated
292 as the ratio of a trait's community variance (population-level variance in our case) in relation
293 to its variance observed on the regional scale (the variance observed all along the climatic
294 gradient in our case) assessed at the individual level. This index represents trait values'
295 dispersion and assesses the strength of the environmental filtering in every trait's expression
296 (Violle et al. 2012). Values close to or higher than 1 depict no environmental filtering in the
297 expression of traits, with population-level variances being relatively equal to regional ones.
298 When values are below 1 for a given population, this index denotes that trait expression is less
299 scattered than its heterogeneity on the regional scale. For instance, lower values indicate
300 environmental filtering, which implies that the population-level trait expression is less
301 heterogeneous than the species regional pool of variance. To assess if our climatic gradient
302 was related to trait variances, we established relations with Pearson's correlation in each
303 trait's $T_{IC/IR}$ and PC1.

304 All the statistical analyses were carried out with version 4.1 of the R software (R Core Team
305 2020).

306

307 **Results**

308 Trait adjustments along the gradient

309 We found a positive correlation (i.e. the mean trait values rising towards the gradient's colder
310 and wetter end) between climate (PC1) and HV, the maximum assimilation rate (A_{max}),
311 maximum stomatal conductance (gs_{max}), $\delta^{13}C$ and the predawn leaf water potential (Ψ_{pd}) (Fig.

2, Table S1). On the contrary, we found that PC1 was negatively correlated (i.e. trait values lowering towards the colder and wetter end of the gradient) with xylem-specific conductivity (Ks), WUEi, hydraulically weighted vessel diameter (Dh) and percent loss of conductivity (PLC). We also observed marginally significant negative correlations between PC1 and vessel area per sapwood unit (VA) (Fig. 2, Table S1). LSC and Vd did not significantly correlate with climate. The density curves for the vessel diameters (Fig. 3) revealed that they ranged from 7 to 55 µm. A first peak on the curves for all the populations was observed at 10 µm, with a second one at around 20 µm, which corresponded to their average lumen diameter. The frequency of larger diameters notably decreased in the populations located on the cold-wet extreme of the gradient (i.e. kernel density estimations for the 30 µm diameter-width vessels was around 0.02 in all the populations, except in Vercors and Bauges, with drops to 0.012 and 0.011, respectively).

Trait coordination

Path analyses with the best adjustment included all the traits, except Ψ_{pd} and WUEi, which were rejected by the model (Table 3, Fig. 4). Wood anatomical traits were closely correlated, with Dh positively influencing VA and lowering Vd. Dh was a central trait that significantly increased Ks and LSC. Dh also indirectly influenced HV (Table 3) by promoting a reduction in the leaf area when vessels were narrower. Ks and LSC strongly correlated with HV. PLC significantly increased LSC and positively correlated with HV (Table 3). Of the stem hydraulic traits, only Ks showed a negative relation with gs_{max}. Leaf physiological traits correlated with higher stomatal conductance to promote greater assimilation.

The path analysis for the arid and warm sites (Fig. 4B) depicted a weaker relation among trait groups. A lesser predictive response of Dh was found on Ks, with only a tendency for LSC and of Ks on gs_{max}. The relation between Dh and Vd was not significant in the arid-warm model.

However, only this model depicted a significant direct influence of gs_{max} on $\delta^{13}C$. The path analysis for the wet-cold sites (Fig. 4C) maintained the correlation strength between the wood anatomical and hydraulic traits observed in the analysis for all the traits. However, PLC showed no significant correlation with any trait in this model.

Trait variance patterns

The trait variance analysis performed at the community-level showed that climate significantly correlated with the community-level trait variances in relation to their regional pool ($T_{IC/IR}$) for HV and gs_{max}, and both reduced at the drier and warmer sites (Fig. 5, Table S2). A tendency was noted with strong correlation coefficients for Ks, Dh, and VA (Fig. 5), whose variances lowered at the wetter and colder sites. No significant filtering pattern was found in the community-level variances for the other traits in response to the climatic gradient (Fig. 5, Table S2).

Discussion

Our trait adjustments and coordination results evidence that beech trees follow two different strategies along the gradient to cope with cold temperature or aridity and heat. Both these two strategies are based on the acclimation of xylem hydraulic traits and leaf physiological ones. Interestingly, our outcomes also suggest that climatic extremes modulate the intrapopulation variances of these trait groups, which may affect their plasticity and acclimation capacity to a shifting environment.

Trait adjustments along the gradient

Our results show that as conditions became colder and moister, beech develop more conservative traits related to hydraulic efficiency (i.e. small vessel hydraulic diameter, Dh; and xylem specific conductivity, Ks), while leaf physiology traits adjust to more acquisitive

behaviour (i.e. high gs_{max}, A_{max}, and low water-use efficiency). The drop in Dh is consistent with results from studies showing vessel diameter reductions in cold ecosystems as a prevention mechanism against freeze-thaw cavitation (Castagneri et al. 2015, Schreiber et al. 2015, García-Cervigón et al. 2020). In line with this, several works observe that vessel diameters larger than 30 µm are highly vulnerable to cavitation due to freeze-thaw cycles (Davis et al. 1999, Schreiber et al. 2013, Medeiros and Pockman 2014), and the vessel size of trees adapted to cold conditions tends to go below that threshold (Schreiber et al. 2015). Our results agree with these outcomes because the trees in the coldest populations show a substantially lower frequency of vessels above 30 µm (Fig. 3). These results demonstrate the important selective pressure of low temperatures in northern populations. Nevertheless, the high gas exchange rates (i.e. gs_{max} and A_{max}) at these sites agree with beech's high assimilation capacity in mountainous environments and at high latitudes to compensate for shorter growing seasons (Bresson et al. 2011). This strategy also allows high carbon acquisition and water-use efficiency during early spring when late frosts occur (Huxman et al. 2008, Hernández-Calderón et al. 2014). Along these lines, physiological adjustments that enhance photosynthetic efficiency in colder environments and higher elevations have been reported to promote more positive leaf $\delta^{13}C$ values (Hultine & Marshall, 2000). This agrees with our observed trend of more positive $\delta^{13}C$ towards the cold-wet sites.

Our results unexpectedly show higher HVs (i.e. smaller leaf area per sapwood unit) as climate becomes wetter and colder, which contradicts consistent intraspecific evidence (Pritzkow et al. 2019, Rosas et al. 2019, López et al. 2021). However, our results are similar to those reported by Fuchs et al. (2021), who reported higher HV in Norway maple trees growing in moister climates, but were limited by low hydraulic conductivity. Indeed HV is also known to increase in response to hydraulic efficiency losses to maintain homeostatic water uptake to leaves without risking excessive reductions in water potential (Mencuccini et al. 2019, López et al. 2021). Thus, our results show that HV is considerably mediated by Ks and Dh (Fig. 4, Table 3),

and its unexpected response is likely triggered by the low Ks values at the colder sites. This result is also supported by the non-significant response of leaf-specific hydraulic conductivity (i.e. LSC) along the gradient.

Towards more arid and warmer conditions, beech shifts its leaf physiology to a more conservative strategy (i.e. reductions in gs_{max} and A_{max}, and better water-use efficiency). This potentially prevents excessive dehydration and reduces the cavitation risk at low water potentials. This result agrees with previous works showing high plasticity and acclimation capacity of gas exchange traits in beech (Aranda et al. 2015, Lübbe et al. 2017, Didion-Gency et al. 2021, Martin-Blangy et al. 2021) and other species (Torres-Ruiz et al. 2019, López et al. 2021). However, one surprising finding is that the trees on the arid-warm edge of the gradient have the highest Dh and Ks, which could mean higher dehydration and hydraulic failure risks during drought (Hajek et al. 2014). This situation contradicts previous studies, which show reductions in vessel diameter and Ks in beech populations with increasing aridity (Schuldt et al. 2016, Stojnić et al. 2018). Nonetheless, our results agree with a recent work showing that the hydraulic conductivity and lumen diameters of top *P. sylvestris* branches increase in arid populations with slight carbon input (Kiorapostolou et al. 2020). This adjustment may allow low-productive trees to compensate for reduced whole-tree hydraulic efficiency caused by narrower rings forming at their stem base (Pellizzari et al. 2016, Prendin et al. 2018), and to relocate carbon to other organs to cope with drought (e.g. developing deeper roots) (Eilmann et al. 2009, Matisons et al. 2019). Maintaining a certain hydraulic conductivity level can also optimise water use and carbon assimilation during high water availability periods, despite the higher water stress risk during summer drought (Hajek et al. 2014, Kiorapostolou et al. 2020). Indeed the trees growing at the arid-warm sites display more stress (i.e. more negative predawn water potentials, Ψ_{pd}; a higher percent loss of conductivity, PLC). Nevertheless, their PLC values are low (i.e. mainly < 30%) which suggests that the observed leaf-physiological adjustments successfully buffer the impacts of higher VPD and aridity.

However, maintaining high Ks and Dh can be a risky strategy in the southern populations of our gradient as regards climate change predictions. Previous studies conducted with beech and other species demonstrated that these traits show low plasticity (Eilmann et al. 2014, Hajek et al. 2016, Pritzkow et al. 2019, Torres-Ruiz et al. 2019) and slow responses to environmental changes (Tomasella et al. 2018, Pritzkow et al. 2019). Such limited plasticity in the short term can increase these populations' vulnerability to sudden heat waves and extreme droughts in forthcoming decades. Their short-term fitness might rely on trait adjustments in other organs, such as shifts in leaf physiology, leaf shedding or deeper roots developing. We suggest that future works address the acclimation of water-use strategies and also include root traits (Hertel et al. 2013) to, therefore, provide a more complete understanding of how trees modulate their water economy in response to climate variability.

Trait coordination

Interestingly, our results demonstrate that environmental conditions modulate the correlation between traits, which agrees with the results of Carvalho et al. (2020) and Benavides et al. (2021). Our results also suggest that the relative importance of adjustments at xylem and leaf levels depends on the acting climatic constraint. Trees that grow at sites limited by low temperature show a closer coupling between the xylem anatomical and hydraulic traits. This agrees with the outcomes of Carvalho et al. (2020), who report that *P. sylvestris* trees display more coordination between traits in harsher environments. This reinforces our results about the important selective pressure of the low temperatures at our northern sites, which promotes a specific combination of hydraulic traits to avoid freeze-thaw cavitation and harmful water potentials (i.e. smaller vessel diameter, lower hydraulic conductivity and higher HV).

437 Conversely, trait coordination depicted by the arid-warm model suggests that the acclimation
438 strategy to increasing aridity and heat involves mainly leaf traits through selecting trait
439 combinations to increase water-use efficiency and to minimise water losses. Specifically, dry
440 origin trees show significant increases in leaf-specific conductivity and HV in response to
441 incremented percent loss of conductivity. This coordination denotes a smaller leaf area
442 triggered by PLC, which suggests that they are prone to early leaf shedding under summer
443 conditions. This adjustment reduces trees' transpiration surface and prevents cavitation at
444 high VPD and water depletion (Pivovaroff et al. 2016, Leuschner 2020). Indeed, pre-senescent
445 leaf shedding is reported in beech in July or August if drought conditions are intense enough
446 (Leuschner 2020, Schuldt et al. 2020). Moreover, the negative correlation between gs_{max} and
447 leaf $\delta^{13}C$ depicts marked stomatal control in trees, which limits their gas exchange capacity.
448 This allows them to optimise leaf-level water use upon maximum stomatal conductance, which
449 helps to prevent hydraulic failure (Grossiord et al. 2020). This response falls in line with studies
450 that have observed consistent links between lower $\delta^{13}C$ discrimination and leaf morphological
451 adjustments to limit water loss (large leaf mass per area) (Wright et al. 2005, Rosas et al.
452 2019).

453 It is worth noticing that Dh comes over as a key trait in beech water-use strategies to adapt to
454 climate variability as our results depict that it mediates the response of many other traits (i.e.
455 Vd, VA, Ks, Kl, and HV). The significant negative correlation between Ks and gs_{max} observed in
456 all the path analyses is also noteworthy. This contrasts with the assumptions made that higher
457 xylem water transport capacity promotes incremented leaf-level water use (Brodribb et al.
458 2002, Brodribb and Holbrook 2003, Reich 2014). However, the low leaf-level water use and
459 high water transport capacity of the xylem can also prevent dehydration and maintain a well-
460 hydrated tree status. In this context, stomata at the leaf-level act as a bottleneck for water
461 movement and reduce water depletion during maximum gas exchange periods (Zimmermann
462 2002, Sack and Holbrook 2006). This strategy may be particularly relevant for trees growing in

463 drier environments or those exposed to high seasonality because it can also enhance xylem
464 protection from hydraulic failure caused by low water potentials (Pivovaroff et al. 2014, 2016).
465 For instance, similar adjustments have been reported as an adaptation mechanism to drought
466 in Mediterranean semiarid shrubs, especially in species that operate on low safety margins
467 (Pivovaroff et al. 2014).

468 Overall, these results highlight the variability of the trait combinations that beech can display
469 in response to different environmental conditions, and indicate that the vessel hydraulic
470 diameter is a key trait for modulating the acclimation strategies of beech's water economy.
471 Further research is needed to test whether the observed coordination structures are sustained
472 in other populations limited by high aridity and VPD, and also by low temperatures.

473 Trait variance patterns.

474 Our results show that the climatic extremes in our gradient reduce the variances of gs_{max}, HV,
475 Dh, VA and Ks. These results support previous observations showing that the variances of
476 some traits reduce when climatic conditions become harsher, i.e., climatic filtering (Swenson
477 et al. 2012, Anderegg et al. 2020). We note two response patterns associated with low
478 temperature and aridity that align with the observed individual trait adjustments and
479 coordination along the gradient.

480 The variances of the traits related to water transport efficiency (Dh, VA, Ks) show signs of
481 climatic filtering in the populations growing under moister and colder conditions (i.e. $T_{IC/IR}$ <1).
482 This observation reinforces the notion that such conditions filter out wide vessels to reduce
483 vulnerability to frost-induced cavitation, especially those above the 30 µm threshold. Indeed,
484 this disturbance can be particularly harmful if it takes place early in spring when leaves are
485 already transpiring (Magnani and Borghetti 1995, Lemoine 2001). For instance, frost-induced
486 cavitation in spring has been reported to cause conductivity losses up to 60% in beech
487 (Magnani and Borghetti 1995), which can significantly increase decay and the mortality risk.

These results are consistent with reported patterns of reduced community variances of wood anatomy traits in response to low temperatures (Swenson and Enquist 2007, Swenson et al. 2012). On the contrary, the gs_{max} and HV variances display an opposite pattern by lowering in the populations growing under drier and hotter conditions. This suggests that the high temperatures, VPD and aridity along our gradient select trait values that promote stomatal regulation; i.e. lower leaf-level water use, and maintain water status. It should be noted that although Ks and gs_{max} are closely related according to the path analyses, their divergent variance patterns suggest that the adjustment of gs_{max} in response to higher aridity is uncoupled from hydraulics. Hence selecting a lower gs_{max} may rely on other mechanisms linked with water-use dynamics at the leaf-level, such as stomatal sensitivity, osmotic adjustments or hormonal regulation mechanisms, including aquaporins (Schroeder et al. 2001, Kapilan et al. 2018).

Interestingly, although our previous high Ks and Dh outcomes at drier sites suggest more vulnerability to drought, their wide variance at these sites could be advantageous for the overall population. Firstly because it may depict greater acclimation capacity as these populations would have a wider pool of heritable trait plasticity available (Valladares et al. 2014, Anderegg et al. 2020). This would promote better tolerance to disturbances for some trees, while others would succumb, which would increase populations' chances to remain functional. Secondly, more water transport efficiency diversity could imply higher functional diversity and enhanced resilience against drought or heat waves. For instance, beech has higher growth and growth recovery rates after extreme droughts in more functionally diverse stands (Pretzsch et al. 2013, Mölder and Leuschner 2014). The same positive effect of stand functional diversity on resilience has been confirmed for co-existing *Abies alba* (Gazol and Camarero 2016) and tropical forests (Schmitt et al. 2020). One probable mechanism behind this positive effect is tree complementarity in water use based on root and/or stem hydraulic traits (Gazol and Camarero 2016). Tree complementarity can buffer or slow down soil water

depletion impacts by reducing resource use overlapping and competition (Morin et al. 2011, González de Andrés et al. 2017). However, these studies addressed functional diversity based on species identity in mixed stands. To what extent hydraulic traits' heterogeneity in both monospecific and mixed stands can significantly enhance beech resilience when facing extreme droughts remains unclear. Future studies are needed to further explore this topic and to better understand the influence of population-level trait variances on species acclimation.

Conclusions

This study highlights two main beech responses to climate variability along a temperature and aridity gradient. Colder and moister conditions promote narrower vessels, and greater stomatal and assimilation capacity, which are likely to prevent frost-induced cavitation and to compensate for shorter growing seasons. As climate becomes drier and warmer, the adjustment and coordination of traits are based mainly on leaves to promote reductions in stomatal capacity, increments in water-use efficiency and early leaf shedding. However, the trees at the arid and warm sites still possess high water transport capacity along the xylem and wide vessel diameters. This suggests that acclimation to sudden rises in aridity and temperature relies mainly on leaves to minimise water depletion and to protect the xylem from negative water potentials. At the population-level, the trait variances controlling water transport capacity increase with more arid and hotter conditions. This could be advantageous for the overall populations on the arid-warm end of the gradient. Higher heterogeneity (i.e. plasticity) can increase their acclimation capacity and the chances of some trees better tolerating the impact of extreme droughts. High water-use diversity could also favour tree complementarity and populations' resilience. Intrapopulation variance is, thus, highlighted as a key parameter for gaining a better understanding of species responses to climate change. Future studies are needed to better assess the role of intrapopulation variances in acclimation

processes and their influence on stands' resilience. We also advocate the inclusion of root traits in future research. Assessing traits from all the organs involved in water use will provide a more complete understanding of how tree species acclimate their water-use strategies.

Conflict of interest

The authors declare no conflict of interest.

Acknowledgements

EV was supported by a predoctoral fellowship funded by the Spanish Ministry of Economy and Competitiveness as part of Project HYDROMED (PID2019-111332RB-C21). AV and LM were supported by Projects INERTIA (PID2019-111332RB-C22), and IMAGINA (Prometeu program/2019/110, GVA). L.M. was additionally supported by the Spanish MICINN (PTA2019-018094). AV was also supported by a WSL Visiting Fellowship. MD and CG were supported by the Swiss National Science Foundation (SNF) (PZ00P3_174068) and the Sandoz Family Foundation. We are grateful to the two tree climbers, J. Baudry and E. Norois, for their help during fieldwork. We thank C. Donzé for support in the field and laboratory. The plot design used in this study forms part of the GMAP plot network (https://oreme.org/observation/foret/gmap/), partly funded by the OSU OREME in Montpellier, and by the ANR project BioProFor (contract no. 11-PDOC-030-01). The CEAM foundation is supported by the Generalitat Valenciana.

Authors' contributions

CG, AV and EV designed the study. XM selected the field sites. MD, CG, and EV collected data. MD, AV, LM and EV performed the lab work. EV analysed the data. All the authors contributed critically to the writing of the manuscript, which was led by EV.

References

Ahrens CW, Rymer PD, Tissue DT (2021) Intra-specific trait variation remains hidden in the environment. New Phytologist 229:1183–1185.

Anderegg WRL (2015) Spatial and temporal variation in plant hydraulic traits and their relevance for climate change impacts on vegetation. New Phytologist 205:1008–1014.

Anderegg WRL, Klein T, Bartlett M, Sack L, Pellegrini AFA, Choat B, Jansen S (2016) Meta-analysis reveals that hydraulic traits explain cross-species patterns of drought-induced tree mortality across the globe. 113:5024–5029.

Anderegg LDL, Loy X, Markham IP, Elmer CM, Hovenden MJ, HilleRisLambers J, Mayfield MM (2020) Aridity drives coordinated trait shifts but not decreased trait variance across the geographic range of eight Australian trees. New Phytologist

Aranda I, Cano FJ, Gascó A, Cochard H, Nardini A, Mancha JA, López R, Sánchez-Gómez D (2015) Variation in photosynthetic performance and hydraulic architecture across European beech (Fagus sylvatica L.) populations supports the case for local adaptation to water stress. Tree Physiology 35:34–46.

Benavides R, Carvalho B, Matesanz S, Bastias CC, Cavers S, Escudero A, Fonti P, Martínez-Sancho E, Valladares F (2021) Phenotypes of Pinus sylvestris are more coordinated under local harsher conditions across Europe. Journal of Ecology 109:2580–2596.

583 Bouche PS, Larter M, Domec JC, Burlett R, Gasson P, Jansen S, Delzon S (2014) A broad survey
584 of hydraulic and mechanical safety in the xylem of conifers. Journal of Experimental
585 Botany 65:4419–4431.

586 Bréda Nathalie, Huc Roland, Granier André, Dreyer E (2006) Temperate forest trees and stands
587 under severe drought: a review of ecophysiological responses, adaptation processes and
588 long term consequences. Ann For Sci 63:625–644.

589 Bresson CC, Vitasse Y, Kremer A, Delzon S (2011) To what extent is altitudinal variation of
590 functional traits driven by genetic adaptation in European oak and beech? Tree
591 Physiology 31:1164–1174.

592 Brodribb TJ, Holbrook NM (2003) Stomatal closure during leaf dehydration, correlation with
593 other leaf physiological traits. Plant Physiology 132:2166–2173.

594 Brodribb TJ, Holbrook NM, Gutiérrez M v. (2002) Hydraulic and photosynthetic co-ordination in
595 seasonally dry tropical forest trees. Plant, Cell and Environment 25:1435–1444.

596 Capblancq T, Morin X, Gueguen M, Renaud J, Lobreaux S, Bazin E (2020) Climate-associated
597 genetic variation in Fagus sylvatica and potential responses to climate change in the
598 French Alps. Journal of Evolutionary Biology 33:783–796.

599 Carvalho B, Bastias CC, Escudero A, Valladares F, Benavides R (2020) Intraspecific perspective
600 of phenotypic coordination of functional traits in Scots pine. PLoS ONE 15

601 Castagneri D, Petit G, Carrer M (2015) Divergent climate response on hydraulic-related xylem
602 anatomical traits of Picea abies along a 900-m altitudinal gradient. Tree Physiology
603 35:1378–1387.

604 Charrier G, Nolf M, Leitinger G, Charra-Vaskou K, Losso A, Tappeiner U, Améglio T, Mayr S
605 (2017) Monitoring of freezing dynamics in trees: A simple phase shift causes complexity.
606 Plant Physiology 173:2196–2207.

607 Cochard H, G Damour, C Bodet, I Tharwat, M Poirier, T Améglio (2005) Evaluation of a new
608 centrifuge technique for rapid generation of xylem vulnerability curves. Physiologia
609 Plantarum 124:410–418.

610 Csardi G, Nepusz T (2006) The igraph software package for complex network research.
611 InterJournal, Complex Systems 1695. http://igraph.org

612 Davis SD, Sperry JS, Hacke UG (1999) The relationship between xylem conduit diameter and
613 cavitation caused by freezing. American Journal of Botany 86:1367–1372.

614 Didion-Gency M, Bachofen C, Buchmann N, Gessler A, Morin X, Vicente E, Vollenweider P,
615 Grossiord C (2021) Interactive effects of tree species mixture and climate on foliar and
616 woody trait variation in a widely distributed deciduous tree. Functional Ecology:1–12.

617 Domec JC, Gartner BL (2002) How do water transport and water storage differ in coniferous
618 earlywood and latewood? Journal of Experimental Botany 53:2369–2379.

619 Ehleringer J, Hall A, Farquhar G (eds) (1993) Stable isotopes and plant carbon-water relations.
620 Academic Press, San Diego.

621 Eilmann B, Sterck F, Wegner L, de Vries SMG, von Arx G, Mohren GMJ, den Ouden J, Sass-
622 Klaassen U (2014) Wood structural differences between northern and southern beech
623 provenances growing at a moderate site. Tree Physiology 34:882–893.

624 Eilmann B, Zweifel R, Buchmann N, Fonti P, Rigling A (2009) Drought-induced adaptation of the
625 xylem in Scots pine and pubescent oak. Tree Physiology 29:1011–1020.

626 Epskamp S (2019) Path Diagrams and Visual Analysis of Various SEM Packages' Output. R
627 package version 1.1.2. https://cran.r-project.org/package=semPlot

628 Farquhar G (1989) Models of integrated photosynthesis of cells and leaves. Philosophical
629 Transactions of the Royal Society of London B, Biological Sciences 323:357–367.

630 Fick SE, Hijmans RJ (2017) WorldClim 2: new 1-km spatial resolution climate surfaces for global
631 land areas. International Journal of Climatology 37:4302–4315.

632 Friedrichs DA, Trouet V, Büntgen U, Frank DC, Esper J, Neuwirth B, Löffler J (2009) Species-
633 specific climate sensitivity of tree growth in Central-West Germany. Trees - Structure and
634 Function 23:729–739.

635 Fuchs S, Leuschner C, Mathias Link R, Schuldt B (2021) Hydraulic variability of three temperate
636 broadleaf tree species along a water availability gradient in central Europe. New
637 Phytologist 231:1387–1400.

638 García-Cervigón AI, Fajardo A, Caetano-Sánchez C, Camarero JJ, Olano JM (2020) Xylem
639 anatomy needs to change, so that conductivity can stay the same: Xylem adjustments
640 across elevation and latitude in Nothofagus pumilio. Annals of Botany 125:1101–1112.

641 García-Cervigón AI, Olano JM, von Arx G, Fajardo A (2018) Xylem adjusts to maintain efficiency
642 across a steep precipitation gradient in two coexisting generalist species. Annals of
643 Botany 122:461–472.

644 Gärtner H, Lucchinetti S, Schweingruber FH (2014) New perspectives for wood anatomical
645 analysis in dendrosciences: The GSL1-microtome. Dendrochronologia 32:47–51.
646 http://dx.doi.org/10.1016/j.dendro.2013.07.002

647 Gazol A, Camarero JJ (2016) Functional diversity enhances silver fir growth resilience to an
648 extreme drought. Journal of Ecology 104:1063–1075.

649 Gazol A, Camarero JJ, Colangelo M, de Luis M, Martínez del Castillo E, Serra-Maluquer X (2019)
650 Summer drought and spring frost, but not their interaction, constrain European beech
651 and Silver fir growth in their southern distribution limits. Agricultural and Forest
652 Meteorology 278

653 Geßler A, Keitel C, Kreuzwieser J, Matyssek R, Seiler W, Rennenberg H (2007) Potential risks for
654 European beech (Fagus sylvatica L.) in a changing climate. Trees - Structure and Function
655 21:1–11.

656 Gleason SM, Butler DW, Waryszak P (2013) Shifts in leaf and stem hydraulic traits across aridity
657 gradients in eastern Australia. International Journal of Plant Sciences 174:1292–1301.

658 González de Andrés E, Seely B, Blanco JA, Imbert JB, Lo YH, Castillo FJ (2017) Increased
659 complementarity in water-limited environments in Scots pine and European beech
660 mixtures under climate change. Ecohydrology 10:1–14.

661 Grossiord C, Buckley TN, Cernusak LA, Novick KA, Poulter B, Siegwolf RTW, Sperry JS, McDowell
662 NG (2020) Plant responses to rising vapor pressure deficit. New Phytologist:nph.16485.
663 https://onlinelibrary.wiley.com/doi/abs/10.1111/nph.16485

664 Hajek P, Kurjak D, von Wühlisch G, Delzon S, Schuldt B (2016) Intraspecific variation in wood
665 anatomical, hydraulic, and foliar traits in ten European beech provenances differing in
666 growth yield. Frontiers in Plant Science 7:1–14.

667 Hajek P, Leuschner C, Hertel D, Delzon S, Schuldt B (2014) Trade-offs between xylem hydraulic
668 properties, wood anatomy and yield in Populus. Tree Physiology 34:744–756.

669 Henry C, John GP, Pan R, Bartlett MK, Fletcher LR, Scoffoni C, Sack L (2019) A stomatal safety-
670 efficiency trade-off constrains responses to leaf dehydration. Nature Communications 10

671 Hernández-Calderón E, Méndez-Alonzo R, Martínez-Cruz J, González-Rodríguez A, Oyama K
672 (2014) Altitudinal changes in tree leaf and stem functional diversity in a semi-tropical
673 mountain. Journal of Vegetation Science 25:955–966.

674 Hertel D, Strecker T, Müller-Haubold H, Leuschner C (2013) Fine root biomass and dynamics in
675 beech forests across a precipitation gradient - Is optimal resource partitioning theory
676 applicable to water-limited mature trees? Journal of Ecology 101:1183–1200.

677 Hultine, K. R., & Marshall, J. D. (2000). International Association for Ecology Altitude Trends in
678 Conifer Leaf Morphology and Stable Carbon Isotope Composition. Oecologia, 123(1), 32–
679 40.

680 Huxman TE, Barron-Gafford G, Gerst KL, Angert AL, Tyler AP, Lawrence Venable AD (2008)
681 Photosynthetic resource-use efficiency and demographic variability in desert winter
682 annual plants.

683 Jourdan M, Kunstler G, Morin X (2019) How neighbourhood interactions control the temporal
684 stability and resilience to drought of trees in mountain forests. Journal of Ecology:1–12.

685 Jourdan M, Lebourgeois F, Morin X (2019) The effect of tree diversity on the resistance and
686 recovery of forest stands in the French Alps may depend on species differences in
687 hydraulic features. Forest Ecology and Management 450:117486.
688 https://doi.org/10.1016/j.foreco.2019.117486

689 Jourdan M, Piedallu C, Baudry J, Defossez E, Morin X (2020) Tree diversity and the temporal
690 stability of mountain forest productivity: testing the effect of species composition,
691 through asynchrony and overyielding. European Journal of Forest Research 140:273–286.
692 https://doi.org/10.1007/s10342-020-01329-w

693 Jourdan M, Piedallu C, Baudry J, Defossez E, Morin X (2021) Tree diversity and the temporal
694 stability of mountain forest productivity: testing the effect of species composition,
695 through asynchrony and overyielding.

696 Jung V, Albert CH, Violle C, Kunstler G, Loucougaray G, Spiegelberger T (2014) Intraspecific trait
697 variability mediates the response of subalpine grassland communities to extreme
698 drought events. Journal of Ecology 102:45–53.

699 Kapilan R, Vaziri M, Zwiazek JJ (2018) Regulation of aquaporins in plants under stress.
700 Biological Research 51:1–11. https://doi.org/10.1186/s40659-018-0152-0

701 Kiorapostolou N, Camarero JJ, Carrer M, Sterck F, Brigita B, Sangüesa-Barreda G, Petit G (2020)
702 Scots pine trees react to drought by increasing xylem and phloem conductivities. Tree
703 Physiology 40:774–781.

704 Klein T (2015) Drought-induced tree mortality: From discrete observations to comprehensive
705 research. Tree Physiology 35:225–228.

706 Kurz WA, Dymond CC, Stinson G, Rampley GJ, Neilson ET, Carroll AL, Ebata T, Safranyik L (2008)
707 Mountain pine beetle and forest carbon feedback to climate change. Nature 452:987–
708 990.

709 Lemoine D (2001) Mechanisms of xylem recovery from winter embolism in Fagus sylvatica.
710 Tree Physiology 21:27–33.

711 Leuschner C (2020) Drought response of European beech (Fagus sylvatica L.)—A review.
712 Perspectives in Plant Ecology, Evolution and Systematics 47:125576.
713 https://doi.org/10.1016/j.ppees.2020.125576

714 Linhart YB, Grant MC (1996) Evolutionary significance of local genetic differentiation in plants.
715 Annual Review of Ecology and Systematics 27:237–277.

716 Lübbe T, Schuldt B, Leuschner C (2017) Acclimation of leaf water status and stem hydraulics to
717 drought and tree neighbourhood: Alternative strategies among the saplings of five
718 temperate deciduous tree species. Tree Physiology 37:456–468.

719 López R, Cano FJ, Martin-StPaul NK, Cochard H, Choat B (2021) Coordination of stem and leaf
720 traits define different strategies to regulate water loss and tolerance ranges to aridity.
721 New Phytologist 230:497–509.

722 Magnani F, Borghetti M (1995) Interpretation of seasonal changes of xylem embolism and
723 plant hydraulic resistance in Fagus sylvatica. Plant, Cell & Environment 18:689–696.

724 Martin-Blangy S, Charru M, Gérard S, Jactel H, Jourdan M, Morin X, Bonal D (2021) Mixing
725 beech with fir or pubescent oak does not help mitigate drought exposure at the limit of
726 its climatic range. Forest Ecology and Management 482

727 Martínez-Vilalta J, Cochard H, Mencuccini M, Sterck F, Herrero A, Korhonen JFJ, Llorens P,
728 Nikinmaa E, Nolè A, Poyatos R, Ripullone F, Sass-Klaassen U, Zweifel R (2009) Hydraulic
729 adjustment of Scots pine across Europe. New Phytologist 184:353–364.

730 Matisons R, Krišāns O, Kārkliņa A, Adamovičs A, Jansons Ā, Gärtner H (2019) Plasticity and
731 climatic sensitivity of wood anatomy contribute to performance of eastern Baltic
732 provenances of Scots pine. Forest Ecology and Management 452

733 Mayr S, Gruber A, Bauer H (2003) Repeated freeze-thaw cycles induce embolism in drought
734 stressed conifers (Norway spruce, stone pine). Planta 217:436–441.

735 McDowell N, Pockman WT, Allen CD, Breshears DD, Cobb N, Kolb T, Plaut J, Sperry J, West A,
736 Williams DG, Yepez EA (2008) Mechanisms of plant survival and mortality during drought:
737 Why do some plants survive while others succumb to drought? New Phytologist 178:719–
738 739.

739 Medeiros JS, Pockman WT (2014) Freezing regime and trade-offs with water transport
740 efficiency generate variation in xylem structure across diploid populations of Larrea sp.
741 (Zygophyllaceae). American Journal of Botany 101:598–607.

742 Mencuccini M, Rosas T, Rowland L, Choat B, Cornelissen H, Jansen S, Kramer K, Lapenis A,
743 Manzoni S, Niinemets Ü, Reich P, Schrodt F, Soudzilovskaia N, Wright IJ, Martínez-Vilalta J
744 (2019) Leaf economics and plant hydraulics drive leaf : wood area ratios. New Phytologist
745 224:1544–1556.

746 Messier J, Lechowicz MJ, McGill BJ, Violle C, Enquist BJ (2017) Interspecific integration of trait
747 dimensions at local scales: the plant phenotype as an integrated network. Journal of
748 Ecology 105:1775–1790.

749 Messier J, Violle C, Enquist BJ, Lechowicz MJ, McGill BJ (2018) Similarities and differences in
750 intrapopulation trait correlations of co-occurring tree species: consistent water-use
751 relationships amid widely different correlation patterns. American Journal of Botany
752 105:1477–1490.

753 Mölder I, Leuschner C (2014) European beech grows better and is less drought sensitive in
754 mixed than in pure stands: Tree neighbourhood effects on radial increment. Trees -
755 Structure and Function 28:777–792.

756 Molina-Montenegro MA, Naya DE (2012) Latitudinal Patterns in Phenotypic Plasticity and
757 Fitness-Related Traits: Assessing the Climatic Variability Hypothesis (CVH) with an
758 Invasive Plant Species. PLoS ONE 7:23–28.

759 Morin X, Fahse L, Scherer-Lorenzen M, Bugmann H (2011) Tree species richness promotes
760 productivity in temperate forests through strong complementarity between species.
761 Ecology Letters 14:1211–1219.

762 Pellizzari E, Camarero JJ, Gazol A, Sangüesa-Barreda G, Carrer M (2016) Wood anatomy and
763 carbon-isotope discrimination support long-term hydraulic deterioration as a major cause
764 of drought-induced dieback. Global Change Biology 22:2125–2137.

765 Pivovaroff AL, Pasquini SC, de Guzman ME, Alstad KP, Stemke JS, Santiago LS (2016) Multiple
766 strategies for drought survival among woody plant species. Functional Ecology 30:517–
767 526.

768 Pivovaroff AL, Sack L, Santiago LS (2014) Coordination of stem and leaf hydraulic conductance
769 in southern California shrubs: a test of the hydraulic segmentation hypothesis. New
770 Phytologist 203:842–850. http://doi.wiley.com/10.1111/nph.12850

771 Poorter H, Lambers H, Evans JR (2014) Trait correlation networks: a whole-plant perspective on
772 the recently criticized leaf economic spectrum. New Phytologist 201:378–382.
773 www.newphytologist.com

774 Prendin AL, Mayr S, Beikircher B, von Arx G, Petit G (2018) Xylem anatomical adjustments
775 prioritize hydraulic efficiency over safety as Norway spruce trees grow taller. Tree
776 Physiology 38:1088–1097.

777 Pretzsch H, Schütze G, Uhl E (2013) Resistance of European tree species to drought stress in
778 mixed versus pure forests: Evidence of stress release by inter-specific facilitation. Plant
779 Biology 15:483–495.

780 Pritzkow C, Williamson V, Szota C, Trouvé R, Arndt SK (2019) Phenotypic plasticity and genetic
781 adaptation of functional traits influences intra-specific variation in hydraulic efficiency
782 and safety. Tree Physiology:1–15.

783 R Core Team (2020) R: A language and environment for statistical computing. R Foundation for
784 Statistical Computing, Vienna, Austria.

785 Reich PB (2014) The world-wide "fast-slow" plant economics spectrum: A traits manifesto.
786 Journal of Ecology 102:275–301.

787 Rosas T, Mencuccini M, Barba J, Cochard H, Saura-Mas S, Martínez-Vilalta J (2019) Adjustments
788 and coordination of hydraulic, leaf and stem traits along a water availability gradient.
789 New Phytologist 223:632–646.

790 Roseel Yves (2012) lavaan: An R Package for Structural Equation Modeling. Journal of Statistical
791 Software 48:1–36. http://www.jstatsoft.org/v48/i02/.

792 Sack L, Holbrook NM (2006) Leaf hydraulics. Annual Review of Plant Biology 57:361–381.

793 Schmitt S, Maréchaux I, Chave J, Fischer FJ, Piponiot C, Traissac S, Hérault B (2020) Functional
794 diversity improves tropical forest resilience: Insights from a long-term virtual experiment.
795 Journal of Ecology 108:831–843.

796 Schreiber SG, Hacke UG, Hamann A (2015) Variation of xylem vessel diameters across a climate
797 gradient: Insight from a reciprocal transplant experiment with a widespread boreal tree.
798 Functional Ecology 29:1392–1401.

799 Schreiber SG, Hamann A, Hacke UG, Thomas BR (2013) Sixteen years of winter stress: An
800 assessment of cold hardiness, growth performance and survival of hybrid poplar clones at
801 a boreal planting site. Plant, Cell and Environment 36:419–428.

802 Schroeder JI, Allen GJ, Hugouvieux V, Kwak JM, Waner D (2001) Guard cell signal transduction.
803 Annual Review of Plant Physiology and Plant Molecular Biology 52:627–658.

804 Schuldt B, Buras A, Arend M, Vitasse Y, Beierkuhnlein C, Damm A, Gharun M, Grams TEE,
805 Hauck M, Hajek P, Hartmann H, Hiltbrunner E, Hoch G, Holloway-Phillips M, Körner C,
806 Larysch E, Lübbe T, Nelson DB, Rammig A, Rigling A, Rose L, Ruehr NK, Schumann K,
807 Weiser F, Werner C, Wohlgemuth T, Zang CS, Kahmen A (2020) A first assessment of the
808 impact of the extreme 2018 summer drought on Central European forests. Basic and
809 Applied Ecology 45:86–103.

810 Schuldt B, Knutzen F, Delzon S, Jansen S, Müller-Haubold H, Burlett R, Clough Y, Leuschner C
811 (2016) How adaptable is the hydraulic system of European beech in the face of climate
812 change-related precipitation reduction? New Phytologist

813 Siefert A, Violle C, Chalmandrier L, Albert CH, Taudiere A, Fajardo A, Aarssen LW, Baraloto C,
814 Carlucci MB, Cianciaruso M v., de L. Dantas V, de Bello F, Duarte LDS, Fonseca CR,
815 Freschet GT, Gaucherand S, Gross N, Hikosaka K, Jackson B, Jung V, Kamiyama C,

816 Katabuchi M, Kembel SW, Kichenin E, Kraft NJB, Lagerström A, Bagousse-Pinguet Y le, Li Y,
817 Mason N, Messier J, Nakashizuka T, Overton JM, Peltzer DA, Pérez-Ramos IM, Pillar VD,
818 Prentice HC, Richardson S, Sasaki T, Schamp BS, Schöb C, Shipley B, Sundqvist M, Sykes
819 MT, Vandewalle M, Wardle DA (2015) A global meta-analysis of the relative extent of
820 intraspecific trait variation in plant communities. Ecology Letters 18:1406–1419.

821 Silverman B (1986) Density Estimation for Statistics and Data Analysis. Chapman and Hall,
822 London.

823 Šímová I, Rueda M, Hawkins BA (2017) Stress from cold and drought as drivers of functional
824 trait spectra in North American angiosperm tree assemblages. Ecology and Evolution
825 7:7548–7559.

826 Sperry JS, Hacke UG (2004) Analysis of circular bordered pit function I. Angiosperm vessels with
827 homogenous pit membranes. American Journal of Botany 91:369–385.

828 Sperry JS, Meinzer FC, McCulloh KA (2008) Safety and efficiency conflicts in hydraulic
829 architecture: Scaling from tissues to trees. Plant, Cell and Environment 31:632–645.

830 Stojnić S, Suchocka M, Benito-Garzón M, Torres-Ruiz JM, Cochard H, Bolte A, Cocozza C,
831 Cvjetković B, de Luis M, Martinez-Vilalta J, Ræbild A, Tognetti R, Delzon S (2018) Variation
832 in xylem vulnerability to embolism in European beech from geographically marginal
833 populations. Tree Physiology 38:173–185.

834 Swenson NG, Enquist BJ (2007) Ecological and evolutionary determinants of a key plant
835 functional trait: Wood density and its community-wide variation across latitude and
836 elevation. American Journal of Botany 94:451–459.

837 Swenson NG, Enquist BJ, Pither J, Kerkhoff AJ, Boyle B, Weiser MD, Elser JJ, Fagan WF, Forero-
838 Montaña J, Fyllas N, Kraft NJB, Lake JK, Moles AT, Patiño S, Phillips OL, Price CA, Reich PB,
839 Quesada CA, Stegen JC, Valencia R, Wright IJ, Wright SJ, Andelman S, Jørgensen PM,

Lacher TE, Monteagudo A, Núñez-Vargas MP, Vasquez-Martínez R, Nolting KM (2012) The biogeography and filtering of woody plant functional diversity in North and South America. Global Ecology and Biogeography 21:798–808.

Tomasella M, Beikircher B, Häberle KH, Hesse B, Kallenbach C, Matyssek R, Mayr S (2018) Acclimation of branch and leaf hydraulics in adult Fagus sylvatica and Picea abies in a forest through-fall exclusion experiment. Tree Physiology 38:198–211.

Torres-Ruiz JM, Kremer A, Carins Murphy MR, Brodribb T, Lamarque LJ, Truffaut L, Bonne F, Ducousso A, Delzon S (2019) Genetic differentiation in functional traits among European sessile oak populations. Tree Physiology 39:1736–1749.

Umaña MN, Swenson NG (2019) Does trait variation within broadly distributed species mirror patterns across species? A case study in Puerto Rico. Ecology 100:1–11.

Valladares F, Gianoli E, Gómez JM (2007) Ecological limits to plant phenotypic plasticity. New Phytologist 176:749–763. http://dx.doi.org/10.1111/j.1469-8137.2007.02275.x

Valladares F, Matesanz S, Guilhaumon F, Araújo MB, Balaguer L, Benito-Garzón M, Cornwell W, Gianoli E, van Kleunen M, Naya DE, Nicotra AB, Poorter H, Zavala MA (2014) The effects of phenotypic plasticity and local adaptation on forecasts of species range shifts under climate change. Ecology Letters 17:1351–1364.

Verryckt LT, van Langenhove L, Ciais P, Courtois EA, Vicca S, Peñuelas J, Stahl C, Coste S, Ellsworth DS, Posada JM, Obersteiner M, Chave J, Janssens IA (2020) Coping with branch excision when measuring leaf net photosynthetic rates in a lowland tropical forest. Biotropica 52:608–615.

Violle C, Enquist BJ, McGill BJ, Jiang L, Albert CH, Hulshof C, Jung V, Messier J (2012) The return of the variance: Intraspecific variability in community ecology. Trends in Ecology and Evolution 27:244–252.

Weigel R, Muffler L, Klisz M, Kreyling J, van der Maaten-Theunissen M, Wilmking M, van der Maaten E (2018) Winter matters: Sensitivity to winter climate and cold events increases towards the cold distribution margin of European beech (Fagus sylvatica L.). Journal of Biogeography 45:2779–2790.

Weiher E, Keddy PA, Kin C (1995) Assembly rules , null models , and trait dispersion: new questions from old patterns. Oikos 74:159–164.

Will RE, Wilson SM, Zou CB, Hennessey TC (2013) Increased vapor pressure deficit due to higher temperature leads to greater transpiration and faster mortality during drought for tree seedlings common to the forest-grassland ecotone. New Phytologist 200:366–374.

Wright IJ, Reich PB, Cornelissen JHC, Falster DS, Groom PK, Hikosaka K, Lee W, Lusk CH, Niinemets Ü, Oleksyn J, Osada N, Poorter H (2005) Modulation of leaf economic traits and trait relationships by climate. Global Ecology and Biogeography:411–421.

Zimmermann MH (2002) Xylem Structure and the Ascent of Sap. Timell TE (ed), 2nd edn. Springer Series in Wood Science.

List of figures

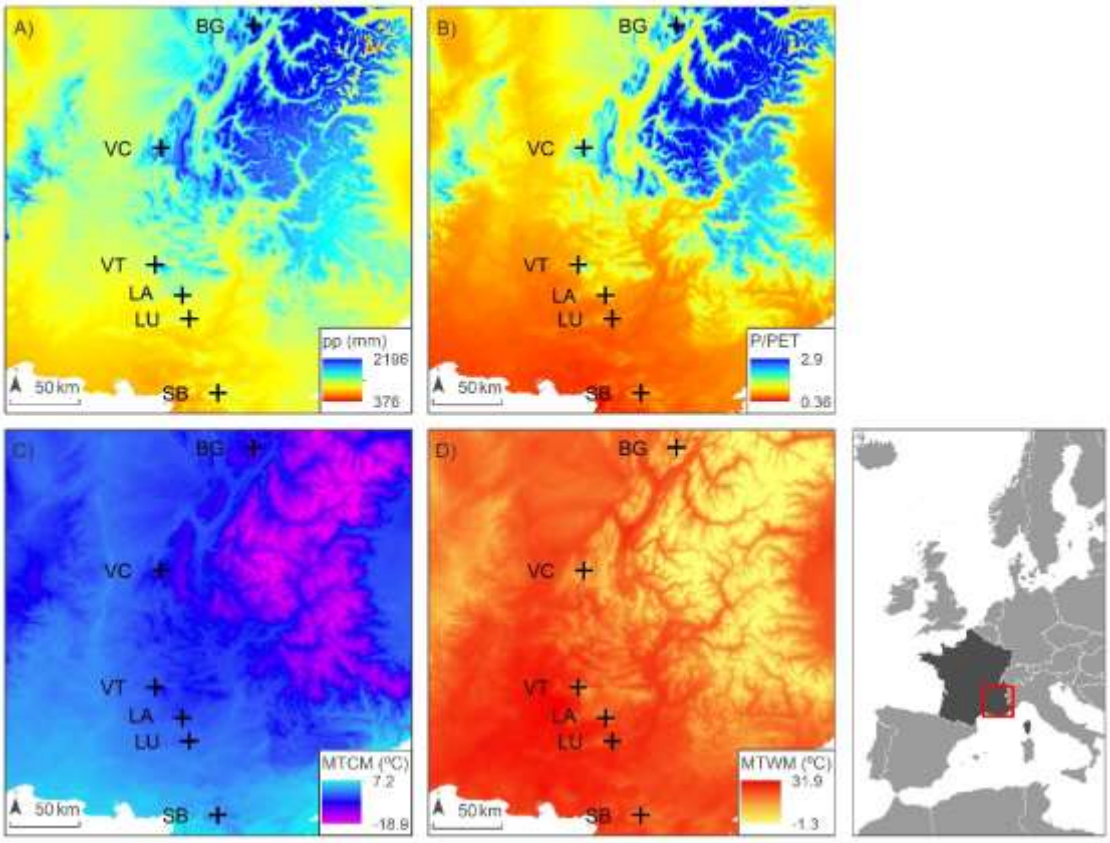

882

883 **Figure 1:** Field site locations and spatial distribution of the main climatic variables

884

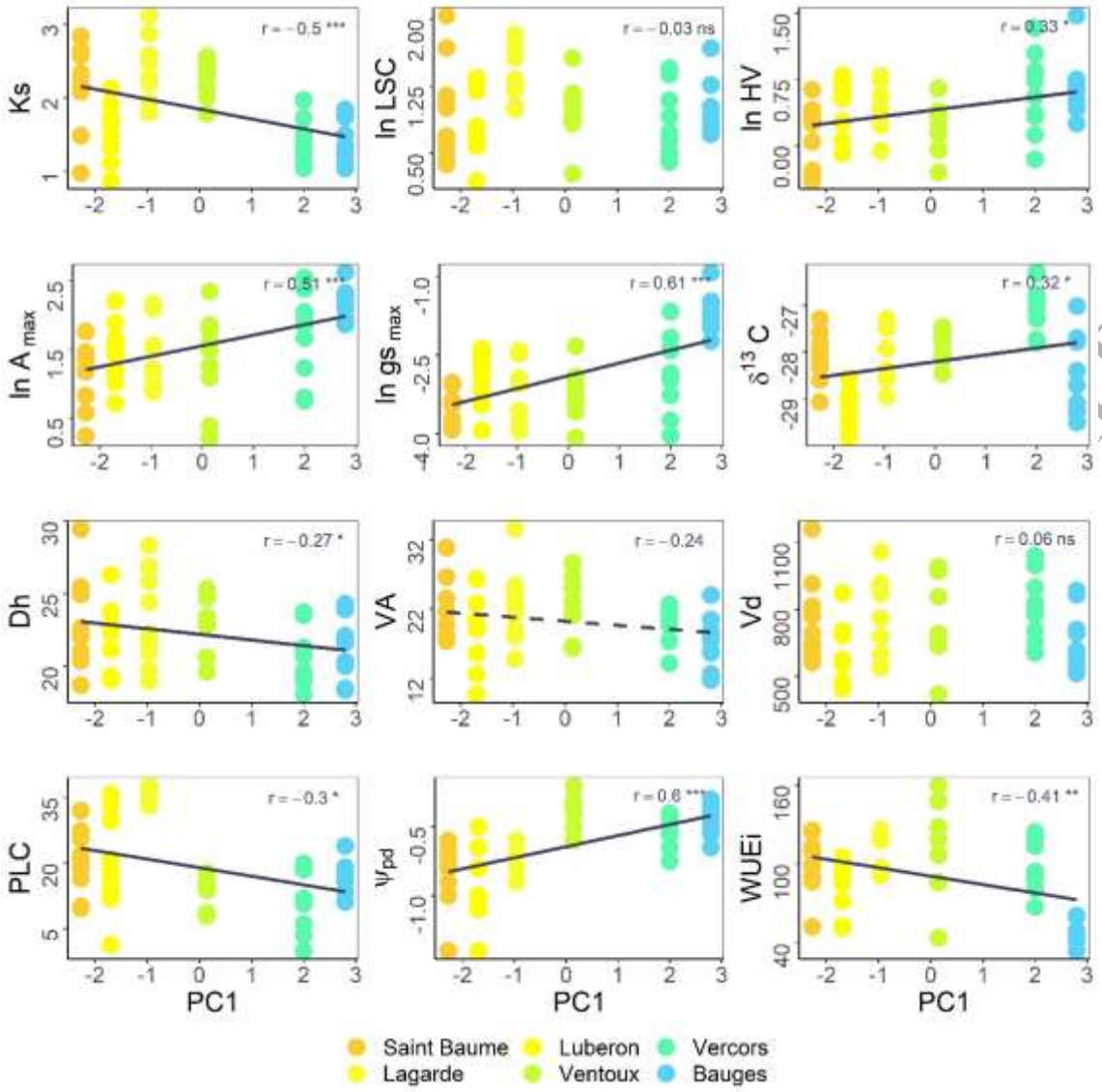

885

886 **Figure 2** Correlations between the measured functional traits and PC1.

887

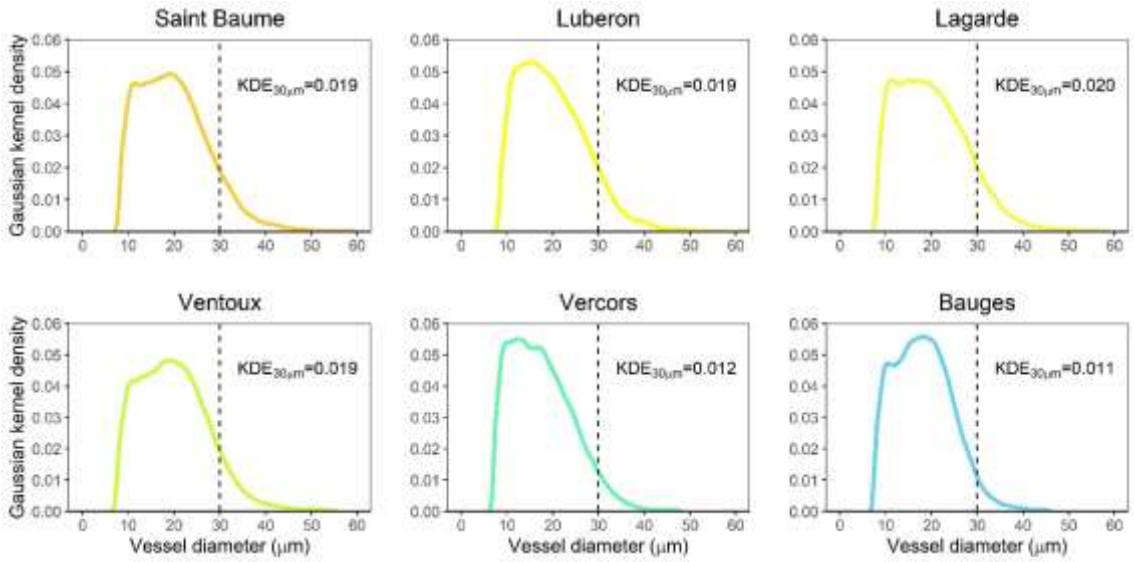

888

889 **Figure 3:** Gaussian kernel density estimates of vessel diameter per population.

890

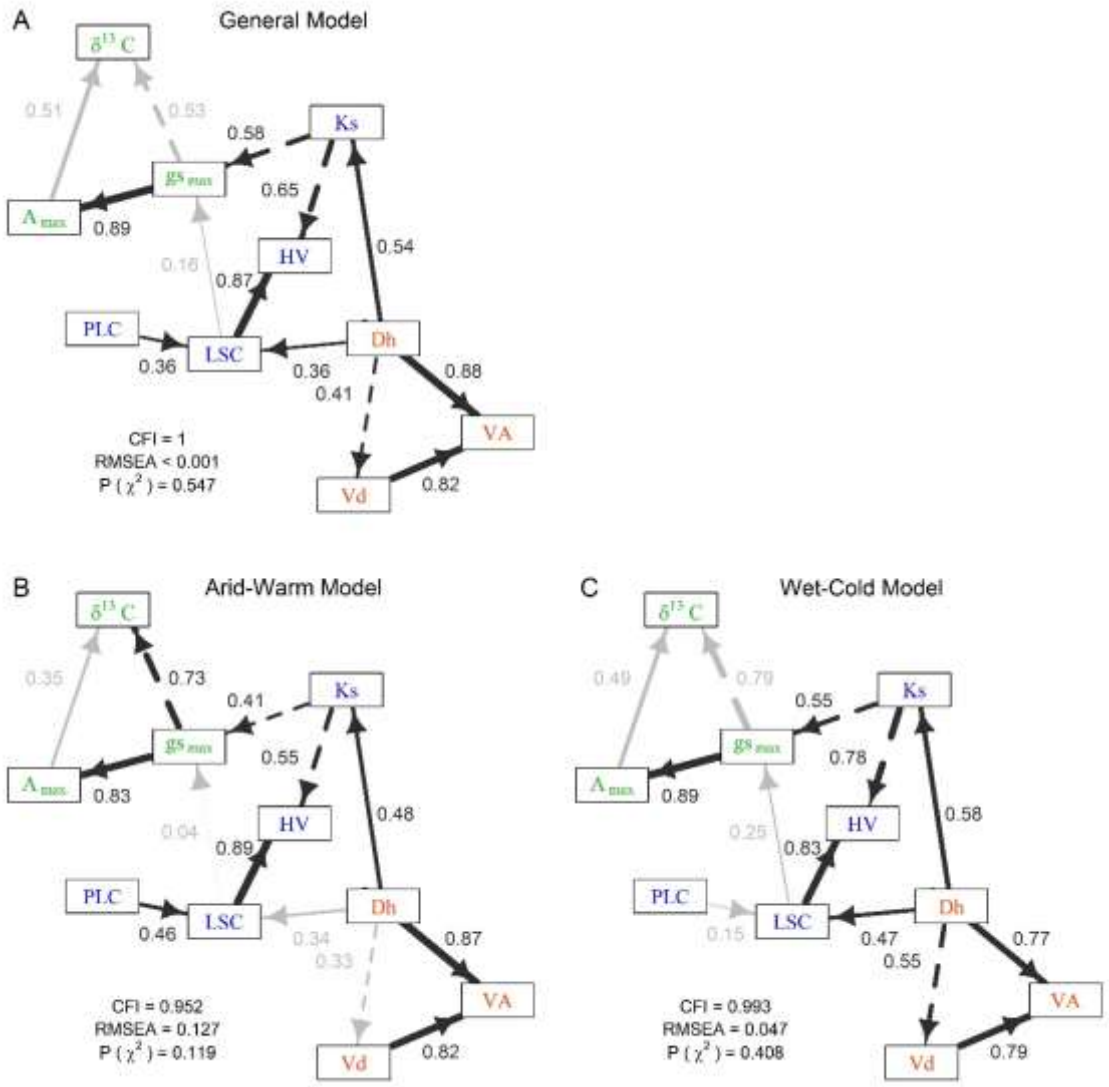

891

892 **Figure 4:** Networks depicting the direct relations between the traits obtained in the path

893 analysis.

894

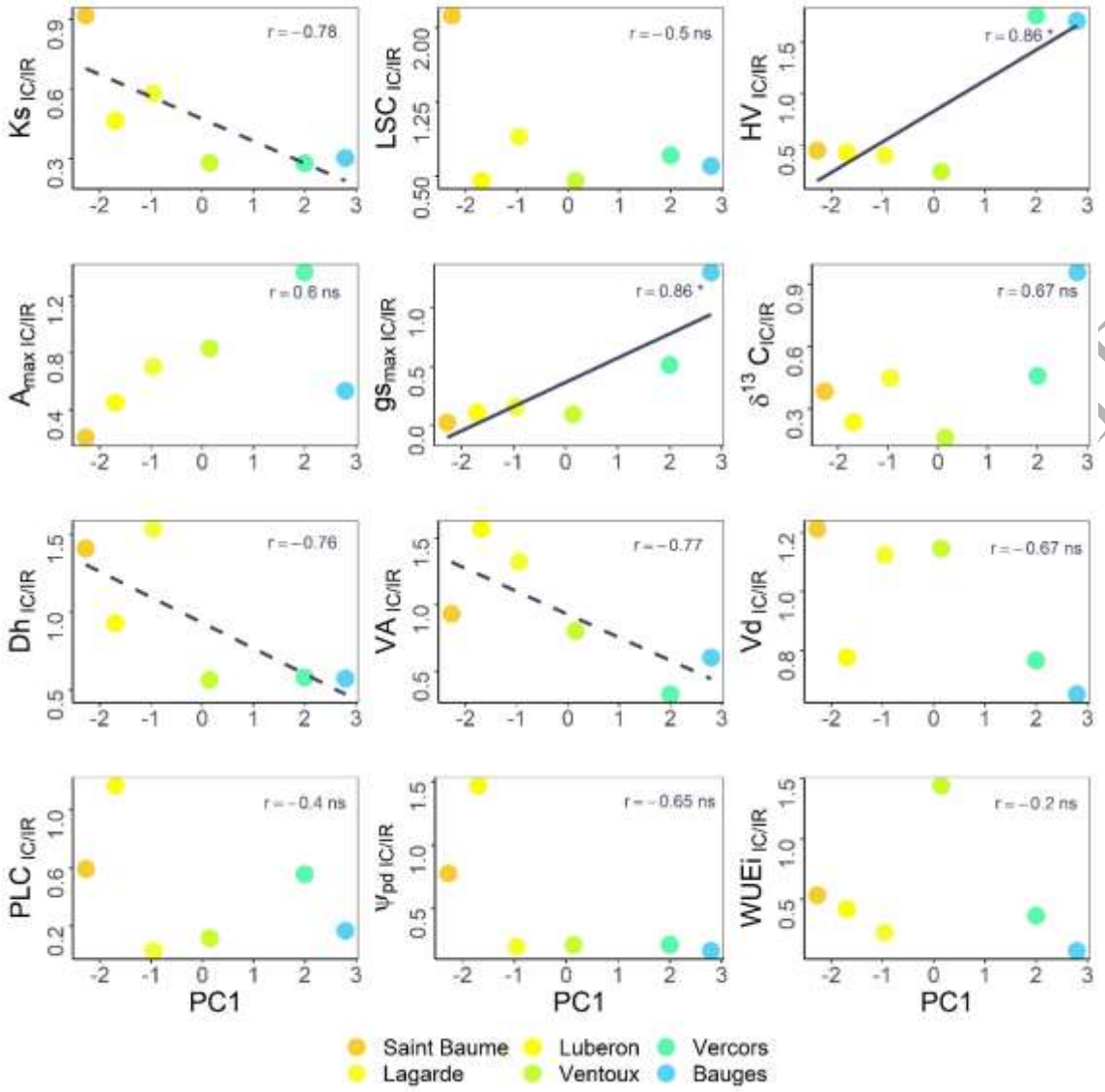

895

896 **Figure 5:** Correlations between the population-level variances of functional traits and PC1.

897

898 **Table 1:** Main attributes of the field sites. MAP, mean annual precipitation; MAT, mean annual
899 temperature; P/PET, precipitation divided by potential evapotranspiration; Lat., latitude; Long.,
900 longitude; Alt., altitude; MTCM, mean minimum temperature of the coldest month; MTWM,
901 mean maximum temperature of the warmest month, DBH, diameter at breast height. Climate

Site Name	Site ID	MAP (mm)	MAT (ºC)	Lat. (ºN)	P/PET (mm)	Long. (ºE)	Alt. (m.a.s.l)	MTCM (ºC)	MTWM (ºC)	Tree height (m)	Tree DBH (cm)
Saint Baume	SB	877	11.0	43.334609	0.65	-5.766041	766	0.8	25	27.6 ± 1.9	49.2 ± 8.7
Luberon	LU	931	10.4	43.819412	0.71	-5.535047	947.5	-0.7	25.6	9.5 ± 0.9	17.52 ± 3.7
Lagarde	LA	1022	9.4	43.973001	0.78	-5.479875	1097.5	-1.9	24.8	12.5 ± 4.6	47.8 ± 17.2
Ventoux	VT	1176	7.9	44.187901	1.13	-5.253608	1299.5	-2.45	22.75	17.15 ± 3.9	32.6 ± 13.5
Vercors	VC	1277	7.0	44.928504	1.23	-5.321516	1301	-4.2	20.95	28.8 ± 2.8	43.3 ± 10.9
Bauges	BG	1292	6.7	45.697930	1.38	-6.214553	1127.5	-4.9	21.05	32.6 ± 2.8	63.4 ± 18.8

902 data derived from the WorldClim database (Fick and Hijmans 2017) .

903

904 **Table 2:** List of studied traits.

Trait	Symbol	Trait group	Units
Percent loss of conductivity	PLC	Xylem hydraulics	%
Xylem-specific conductivity	Ks	Xylem hydraulics	$kg.s^{-1}.m^{-1}.MPa^{-1}$
Leaf-specific conductivity	LSC	Xylem hydraulics	$kg.s^{-1}.m^{-1}.MPa^{-1}$
Huber value	HV	Sapwood/leaf allocation	$cm^2.m^{-2}$
Predawn leaf water potential	Ψ_{pd}	Leaf physiology	MPa
Maximum stomatal conductance	gs_{max}	Leaf physiology /gas exchange	$mmol.m^{-2}.s^{-1}$
Maximum net photosynthesis	A_{max}	Leaf physiology /gas exchange	$\mu mol.m^{-2}.s^{-1}$
Intrinsic water-use efficiency	WUEi	Leaf physiology /gas	Dimensionless

		exchange	
Leaf carbon isotope concentration	$\delta^{13}C$	Leaf physiology /gas exchange	‰
Vessel hydraulic diameter	Dh	Wood anatomy	µm
Vessel density	Vd	Wood anatomy	Vessels.mm^{-2}
Relative vessel lumen area	VA	Wood anatomy	%

905

906 **Table 3:** Estimated path coefficients for the regressions obtained in the three path analyses
907 (degree of significance: ***p<0.001, ** p<0.01, *p<0.05). Significant regressions are depicted
908 in bold. Marginally significant regressions are shown in italics (0.1>p>0.05).

Regressions			General model	Wet-Cold model	Arid-Warm model
VA	~	Dh	**1.466*** **	**1.162*** **	**1.492*** **
VA	~	Vd	**2.221*** **	**1.938*** **	**2.253*** **
Vd	~	Dh	**-0.256****	**-0.337*** **	-0.209
Ks	~	Dh	**0.105*** **	**0.12*** **	**0.085*** **
LSC	~	Dh	**0.053***	**0.059***	*0.054*
LSC	~	PLC	**0.014***	0.007	**0.019****
HV	~	LSC	**1.002*** **	**1.018*** **	**0.986*** **
HV	~	Ks	**-0.564*** **	**-0.585*** **	**-0.552*** **
gs_{max}	~	Ks	**-0.906*** **	**-1.103****	**-0.39***
gs_{max}	~	LSC	0.341	0.812	-0.047
A_{max}	~	gs_{max}	**0.657*** **	**0.6*** **	**0.757*** **
$\delta^{13}C$	~	gs_{max}	-0.529	*-0.663*	**-1.068***
$\delta^{13}C$	~	A_{max}	0.69	0.618	0.563
Indirect regressions					
Dh	~	VA	**-0.569****	**-0.654***	-
Dh	~	HV	**-0.003***	-	-
PLC	~	HV	**0.014***	-	**0.019****

909

910